JOURNAL OF CATALYSIS **161,** 186–193 (1996)
ARTICLE NO. 0175

The Acid Strength of Sulfated Zirconia Measured by Two ^{1}H NMR Techniques in the Presence of Water: 4 K Broad-Line and 300 K High Resolution MAS

Virginie Semmer, Patrice Batamack, Claudine Dorémieux-Morin, Robert Vincent, and Jacques Fraissard

Laboratoire de Chimie des Surfaces, associé au CNRS-URA 1428, Université Pierre et Marie Curie, Casier 196, 4 place Jussieu,
75252 Paris, Cedex 05, France

Received April 3, 1995; revised December 20, 1995; accepted February 2, 1996

The interaction of known concentrations of water molecules with sulfated zirconia has been studied by ^{1}H NMR: broad-line at 4 K and MAS at 300 K. The dependence of the ratio of H_3O^+ to SO_4 groups (H_3O^+/SO_4) on the ratio of adsorbed H_2O to SO_4 (ads. H_2O/SO_4) has been determined; (H_3O^+/SO_4) is equal to 1 when ads. H_2O/SO_4 = 2. The acidity of the sample is directly comparable to that of H_2SO_4, which means that, not being more acidic than H_2SO_4, it cannot really be described as a "superacid." On the basis of the experimental data, the sulfated zirconia sample has been ranked in a previously proposed scale of Brønsted acid strength for solids.

INTRODUCTION

As industry is turning increasingly toward the use of solid acids as catalysts instead of liquid ones, "solid superacids" are being extensively studied (1, 2), especially sulfated zirconia (3–30), using various techniques, some of which entail prior adsorption of a base: Hammett indicator measurements (3–6), XRD (4, 6–14), IR or Raman spectroscopy (6–9, 11–25), XPS (6, 26), ESR (4, 27), HRTEM (8, 9, 19), different gravimetric and calorimetric techniques (5, 11–13, 16, 20, 24), ^{1}H MAS NMR (14, 28), ^{31}P NMR of adsorbed trimethylphosphine (29), and *ab initio* quantum chemical calculations (30).

The use of the quantitative ^{1}H NMR techniques for determining the Brønsted acid strength of solids has been proposed (31–33). Room-temperature ^{1}H MAS NMR of sealed samples, as developed by Pfeifer *et al.* (34, 35), allows the quantitative determination of OH groups of different families on solid surfaces when no adsorbed phase is present. However, the acid strength is not expressed directly by the chemical shift values, which are very sensitive to the presence of hydrogen bonds, mainly because the OH bonds are relatively covalent. In practice, the acid strength of OH groups at a solid surface can be studied only with proton acceptors. We chose water for this purpose. In the presence of hydrogenated adsorbed phases, chemically exchanging H atoms give only one signal under the conditions where ^{1}H MAS NMR can be performed; this technique, therefore, cannot be employed. However, broad-line ^{1}H NMR performed at 4 K, with simulation of the spectra, gives the concentration of the oxyprotonated species formed by the interaction between water and OH groups (31, 32). A scale of Brønsted acid strength has been proposed on the basis of the hydroxonium ion concentrations and/or the strength of hydrogen-bonded species formed (33). The purpose of this paper is to present results obtained on sulfated zirconia using both ^{1}H NMR techniques.

EXPERIMENTAL

As previously noted (4, 18), the catalytic activities of sulfated zirconia depend on the preparation conditions. We chose, therefore, well defined synthesis conditions already optimized for *n*-butane isomerization, considered by Chen *et al.* (4) to correspond to a monolayer of SO_4 groups on the sulfated zirconia surface (maximum coverage of the hydroxide surface).

The conditions adopted are the following (4): (i) Zirconium hydroxide was obtained by dissolving 64.4 g of $ZrOCl_2 \cdot 8H_2O$ in 500 cm^3 of water (0.5 *M*) at room temperature; 28 wt% aqueous NH_4OH was added dropwise with vigorous stirring at room temperature up to a pH of 10; the gel was filtered and washed repeatedly with water until no chlorine ions were detectable and dried at 380 K for 24 h. (ii) For sulfation, 5 g of dry gel was treated with 75 cm^3 of a 0.2 *N* aqueous H_2SO_4 solution for 20 min at room temperature with stirring, filtered without washing, dried at 380 K for 24 h, calcined in a fixed bed furnace in air flow with heating to 820 K at 4 K min^{-1}, maintained 2 h at this temperature, and allowed to cool in air. The tetragonal phase of zirconia is stabilized by sulfation (4, 7, 12), the specific surface area being large (110 m^2 g^{-1}) (4). It is assumed that the above sulfation conditions give a monolayer of H_2SO_4 groups at the zirconia surface (4).

0021-9517/96 $18.00

TABLE 1

Concentration per SO_4 Unit of the Protonated Species after Adsorption of Water Molecules from ^1H Broad-Line NMR Results

	(ads. H_2O)/ SO_4 group ±5%	Formed H_3O^+/ SO_4 group ±10%	Formed ($H_2O\cdots HO$)/ SO_4 group ±10%	Residual OH/SO_4 group ±10%	Residual H_2O/SO_4 group ±10%
a	0.50	No	0.63	1.31	No
b	0.50	No	No	1.95	0.62
a	1.10	0.20	0.89	1.1	No
b	1.10	0.20	No	2.02	0.88
a	1.10[a]	0.27	0.83	0.99	No
b	1.10[a]	0.22	No	1.72	0.90
a	1.50	0.69	0.95	0.26	No
b	1.50	0.64	No	1.22	1.02
a	1.60[a]	0.52	0.95	0.72	No
b	1.60[a]	0.55	No	1.46	1.01
a	2.0	1.05	0.98	0.16	No
b	2.0	1.01	No	1.11	1.02
	3.0	0.84	1.06	0.50	1.00
	3.8	0.89	1.11	0.44	1.67

Note. Letters a or b denote spectra simulations where it is assumed a priori that some (a) or no (b) water molecules hydrogen bond OH groups.

[a] Samples vacuum pretreated at 720 K instead of 570 K.

Following calcination, sulfated zirconia changes only slowly (4). Within 1 week after calcination, 1-g samples were vacuum pretreated with a 24 K h^{-1} heating rate to 570 K (720 K for two samples noted in Tables 1 and 2), maintained 15 h at the maximum temperature and cooled in vacuum. The subsequent procedures have already been described (31–33). Stepwise steaming was performed at 300 K, the maximum water pressure per step being less than one-third of the saturation pressure. The amount of water was checked volumetrically and gravimetrically. Since the water adsorbed in this way is generally not distributed homogeneously, the samples were homogenized at 380 K for 15 h. After cooling they were transferred to narrow thin-walled 5-mm-diameter tubes and sealed; these samples were used for both types of NMR experiment: MAS and broad-line.

The procedures for recording both types of ^1H NMR spectra and simulating broad-line spectra have already been described (31, 32). Some more details are given here. Room temperature MAS was performed with a 400-MHz Bruker spectrometer and 3-kHz spinning of the samples; the repetition time was 20 s for "anhydrous" samples and 5 s if water had been adsorbed. The chemical shifts are expressed relative to an external liquid TMS reference without magnetic susceptibility correction. The H atom concentration corresponding to each of the MAS spectrum signals is based on the contribution of the signal itself and of its spinning side-bands.

For broad-line NMR at 4 K (under "rigid lattice" conditions), the basis of the apparatus is an old cw DP60 Varian spectrometer (1.4092 Tesla) used with a home-made probe. The quality coefficient of the single coil is about 60. The probe can be immersed in liquid helium. Its particularity is that it can be adapted and tuned at the working temperature, using sliding cylindrical capacitors monitored from the outside. Under these conditions, the coaxial wire is no longer part of the active circuit. The sweep of the magnetic field, B_0, is 5×10^{-3} Tesla on the resonance area. The spectra are accumulated as derivatives of the absorption relative to B_0, each scan lasting 100 s with 5 s between scans. In order to obtain derivative spectra, B_0 is modulated at 20 Hz, with a peak to peak amplitude of 5×10^{-5} Tesla. The amplitude of the radiofrequency magnetic field is small (a few 10^{-7} Tesla) to avoid saturation of the resonance. The probe is connected to a 90° power divider/combiner. Phase-sensitive detection was used.

Since the samples are cooled rapidly, they are assumed to be frozen in their 300 K chemical state. This assumption is supported by the following result on antimonic acids (31): it was confirmed that the experimental chemical shift was close to the calculated value, it being assumed that the oxyprotonated species concentrations are those found at 4 K. Moreover, some experiments were performed after adsorption of helium at low pressure: the results are quantitatively the same as without helium, showing that the heat exchange is fast even without helium. Spectra recording begins not less than 30 min after freezing to calm down the turbulences created by the introduction of the probe in the liquid helium. Moreover, this time delay avoids recording during dynamic polarization resulting from a rapid change in the temperature of the sample: this phenomenon, described by Haupt (36), vanishes with time.

ANALYSIS OF ^1H BROAD-LINE NMR DATA

The direct dipolar magnetic interaction between two protons is proportional to r^{-3}, r being the distance between them; it is also directionally dependent on the magnetic field, B_0 (37). Since the dominant contribution to the width of the spectra is that of near-neighbor protons, theoretical absorption functions have been calculated for groups of neighboring H atoms considered as magnetic configurations (37–41), neglecting the much smaller chemical shift effect and the interaction with nuclei not belonging to the groups; the magnetic configurations are assumed to be magnetically isolated from each other. For the models to be used for powder samples, it is also assumed that these configurations are distributed isodirectionally. Each of the corresponding functions is then convoluted by a Gaussian which takes into account the interactions between the hydrogen nuclei of the configuration and those outside this configuration. The other neighboring nuclei with nonzero spins, ^{17}O, ^{33}S, and ^{91}Zr, are in low enough natural abundance for their interactions with ^1H to be neglected. The

TABLE 2

Distance Parameters in pm Used for the Simulation of the ^{1}H Broad-Line NMR Spectra

	(ads. H_2O)/ SO_4 group ±5%	Formed H_3O^+/SO_4 group (pm)			Formed ($H_2O\cdots HO$)/SO_4 group (pm)			Residual OH/SO_4 group (pm)	Residual H_2O/SO_4 group (pm)	
		$r \pm 2$	$r' \pm 3$	$X \pm 5$	$r \pm 2$	$r' \pm 5$	$X \pm 5$	$X \pm 5$ Gaussian	$r \pm 2$	$X \pm 5$
a	0.50		No		165	293	329	329 Gaussian Lorentz. 0.77	No	
b	0.50		No			No		336 Gaussian Lorentz. 0.85	161	320
a	1.10	170		280	165	280	310	Lorentz. 0.80	No	
b	1.10	170		280		No		248 Gaussian Lorentz. 0.88	161	295
a	1.10^a	168		275	165	276	288	Lorentz. 1.0	No	
b	1.10^a	171		279		No		250 Gaussian Lorentz. 1.0	161	280
a	1.50	169		216	163	273	286	Lorentz. 0.88	No	
b	1.50	172		212		No		250 Gaussian Lorentz. 1.08	160	265
a	1.60^a	165		240	164	278	280	Lorentz. 0.93	No	
b	1.60^a	172		210		No		263 Gaussian Lorentz. 0.93	161	268
a	2.0	163	174	205	164	266	280	Lorentz. 0.90	No	
b	2.0	165	177	205		No		245 Gaussian Lorentz. 1.12	160	260
	3.0	161	169	220	163	241	262	232 Gaussian 320 Gaussian	165	215
	3.8	165		221	163	257	280	260 Gaussian 345 Gaussian	165	210

Note. OH group absorption is sometimes described by the derivative of a Lorentzian function whose parameter is in 10^{-4} T. Letters a or b denote spectra simulations where it is assumed a priori that some (a) or no (b) water molecules hydrogen bond OH groups.

[a] Samples vacuum pretreated at 720 K instead of 570 K.

magnetic field parameter of the Gaussian convolution function will be expressed in terms of a spin–spin distance, X, which is close to the shortest distance between a proton of the configuration considered and a proton outside it. Acceptable values of X must be greater than internal H–H distances of the magnetic configurations.

The various species which can be formed when a water molecule interacts with an OH group are shown in Fig. 1. The following magnetic configurations are used to calculate their absorption spectra: (i) an r-dependent two-spin configuration (37) for H_2O ($142 \text{ pm} \leq r \leq 165 \text{ pm}$); (ii) an r-dependent three-spin configuration at the vertices of an equilateral triangle (38, 39) for H_3O^+ ($165 \text{ pm} \leq r \leq 173 \text{ pm}$); (iii) a three-spin magnetic configuration, the spins being located at the apices of an isosceles triangle (40–42) for $H_2O \cdot HOZ$ (Z representing the sulfated zirconia lattice) and H_3O^+ considered as deformed, where r is the base ($142 \text{ pm} \leq r \leq 165 \text{ pm}$) and r' is the length of the equal sides ($1.01 \leq r'/r \leq 1.80$). For OH groups, either a pure Gaussian function or a pure Lorentzian function or a two-spin configuration can be used (43) ($200 \text{ pm} \leq r \leq 300 \text{ pm}$), depending on the OH distribution.

Typical contributions are indicated in Fig. 2. Only half of each centrosymmetrical spectrum is shown in the figures. In practice, broad-line simulated spectra correspond to the weighted sum of 1 to 5 contributions; the corresponding weight parameters range from 0 to 4; the "internal" distance parameters (r and r' values) can be from 1 to 7 and the "external" ones (X values) from 1 to 5. The abscissa scale of each contributing spectrum is related mainly to the r value for the corresponding configuration. The shape of this contribution is related to the number of H atoms of the magnetic configuration and to its other distance parameters, r' and X. In practice, the presence of each chemical species can often be inferred from that of maxima and/or minima of the experimental spectrum at convenient values of the magnetic field. More generally, because of the large number of parameters, we impose an additional

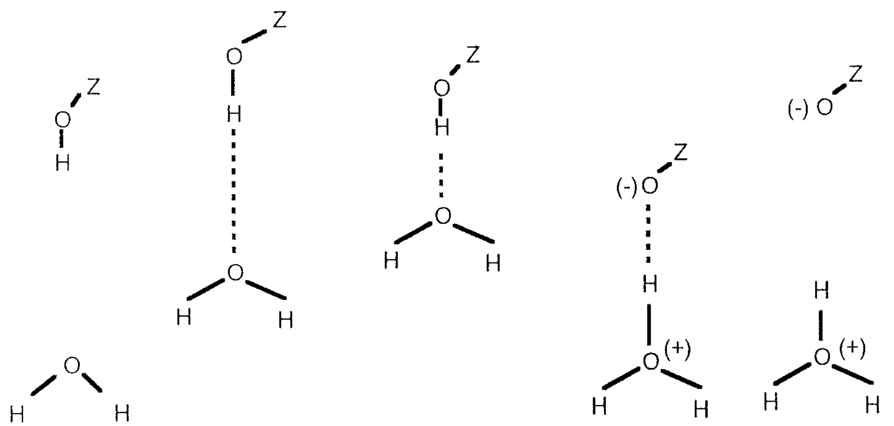

FIG. 1. Possible interactions between a ZOH group (Z belonging to the sulfated zirconia surface) and a water molecule.

condition: the concentrations of the different species must be in agreement with the initial number of acid OH groups; this means that no new water molecule has been formed from OH groups and that no OH group has been obtained by the dissociation of adsorbed water molecules. Except for nonresolved experimental spectra, the concentration of the oxyprotonated species given by the simulation can then be considered as unique. For each sulfated zirconia sample, the single possible simulation satisfied this last condition without being constrained to be so.

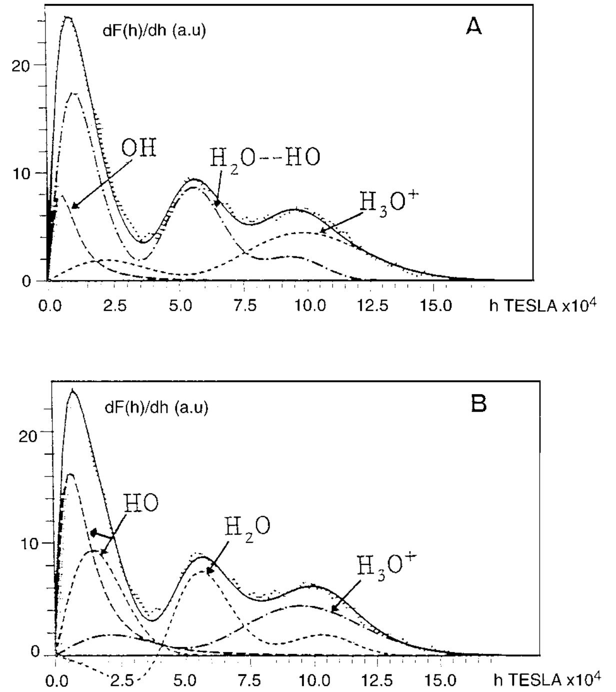

FIG. 2. ^1H Broad-line NMR spectra of hydrated sulfated zirconia at 4 K for ads. $H_2O/SO_4 = 2.0$; h stands for the difference between the applied magnetic field B_0 and the Zeeman resonance field. The simulated spectra A and B (giving the same compositions in this case) are obtained by assuming that, for A, the H atoms of OH groups and of water molecules are at the apices of isosceles triangles, and for B, no first-order magnetic interaction between H atoms of OH groups and of water molecules.

The quality of the fit is appreciated visually. The accuracy on the species concentrations is ±10%. Minimization of the differences between the experimental and calculated spectra has been programmed; it results in a refinement of parameters (especially distance parameters) which is too precise to have any physical significance.

RESULTS

^1H *MAS NMR at 300 K*

The MAS spectra of the sulfated zirconia, calcined in air at 820 K and sealed after vacuum pretreatment without water adsorption, contain the large 600-Hz-wide signal at 5.8 ± 0.2 ppm (Fig. 3A) observed by Riemer *et al.* (14) at 5.85 ppm. There is a second signal at 1.4 ± 0.2 ppm, corresponding to a very small number of H atoms. These signals can be compared with those for zirconia before sulfation: a large one at 4.7 ppm, too wide to be completely narrowed at the MAS spinning rate used (3 kHz) and a small one at 1.5 ppm. Mastikhin *et al.* (28) also observed two signals, at 4.8 and 2.4 ppm, and Riemer *et al.* (14) observed a large one at 3.86 and a small one at 1.60 ppm.

When the number of water molecules per sulfate group adsorbed on sulfated zirconia, ads. H_2O/SO_4, increases, the signal at 5.8 ppm is replaced by another whose chemical shift, denoted δ_E, first decreases (5.4 ppm for ads. $H_2O/SO_4 = 0.5$) and then increases (6.9 and 7.0 ppm for ads. $H_2O/SO_4 = 1.5$ and 2.0, respectively) (Figs. 3B and 3C) before decreasing again (5.7 ppm for ads. $H_2O/SO_4 = 3.8$) (Fig. 3D). The width of this large signal increases to ads. $H_2O/SO_4 = 0.5$ and then decreases to about 2 kHz for ads. $H_2O/SO_4 = 1$ before remaining constant. All the H atoms of the sample resonating at 5.8 ppm before water adsorption are accessible to water. The small signal at 1.4 ppm

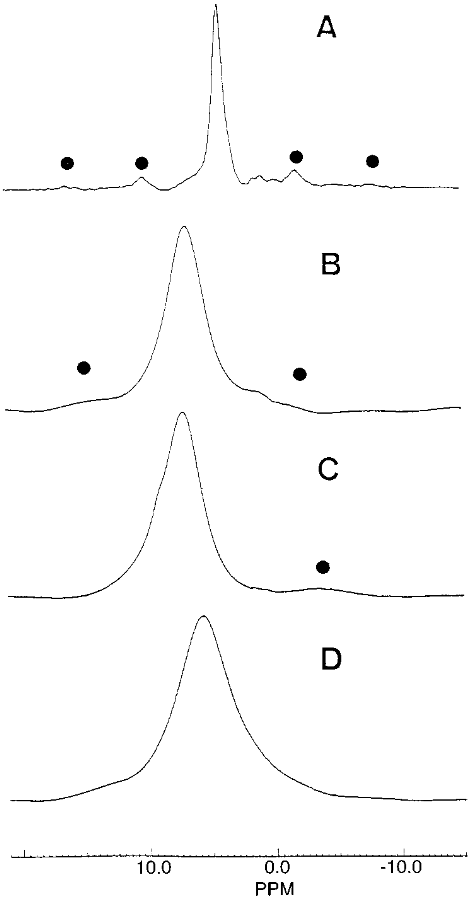

FIG. 3. Examples of ^1H MAS NMR spectra of sulfated zirconia at room temperature, (A) after vacuum pretreatment up to 570 K and (B, C, and D) for ads. $H_2O/SO_4 = 1.5$, 2.0, and 3.8, respectively. Large dots stand for spinning side-bands.

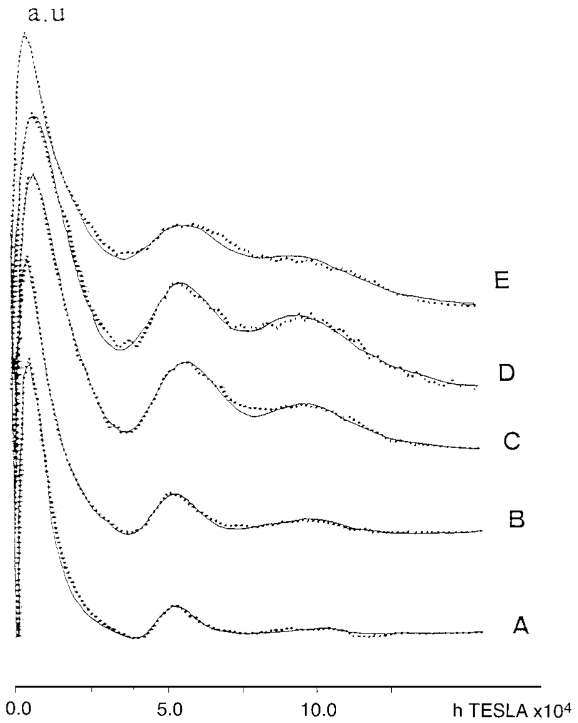

FIG. 4. Examples of ^1H broad-line NMR spectra of hydrated sulfated zirconia at 4 K; h stands for the difference between the applied magnetic field B_0 and the Zeeman resonance field. Dotted lines are for experimental spectra and continuous lines are for simulated spectra using the three-spin isosceles configuration to describe possible interactions between OH groups and water molecules. (A, B, C, D, and E) ads. $H_2O/SO_4 = 0.5$, 1.1, 1.5, 2.0, and 3.8, respectively.

is unchanged whatever the amount of water. The corresponding H atoms are either inaccessible to water or do not interact with it.

In Fig. 3C, for ads. $H_2O/SO_4 = 2.0$, there is a shoulder at about 9 ppm on the main signal (7 ppm); the significance of this signal which corresponds to a relatively small number of H atoms will be discussed later.

^1H *Broad-Line NMR at 4 K*

The broad-line spectra of pretreated samples show no contribution at about $5–6 \times 10^{-4}$ T which could be attributed to water molecules: in agreement with the literature (4) the samples contain only OH groups.

The results for the samples with different concentrations of adsorbed water are normalized to the total number of H atoms per SO_4 group, equal to the sum of twice the number of adsorbed water molecules per SO_4, plus 2.2 (2 from H_2SO_4 plus 0.2 extra OH groups which correspond to the 1.5 ppm MAS peak). The concentrations of the different oxyprotonated species per SO_4 group are reported in Table 1, and the distance parameters used for the simulation are given in Table 2.

The 4 K broad-line spectra of samples after adsorption of water are well resolved (Fig. 4). Hydroxonium ions (whose concentration per sulfate group is denoted H_3O^+/SO_4) are clearly present for ads. $H_2O/SO_4 \geq 1.1$ (Table 1, Figs. 2 and 5). This result is in agreement with that recently stated by Morterra *et al.* (25): these authors claim that IR spectroscopic data indicate surface species ascribable to hydroxonium ions.

For ads. H_2O/SO_4 up to 2, two different simulated spectra were obtained for each ads. H_2O/SO_4 value. The smallest distance between H atoms of OH groups not involved in hydroxonium formation and others belonging to water molecules [denoted r' when a three-spin configuration of protons at the apices of an isosceles triangle is used (Fig. 2A)] goes from 290 to 266 pm when ads. H_2O/SO_4 is increased from 0.5 to 2 (Table 2). Such values suggest that there are no hydrogen bonds between these two kinds of H atom. This can be proved by simulating the experimental spectrum, assuming no first-order magnetic interaction between the corresponding protons, i.e., using "independent" configurations of protons, one with two spins at a distance r

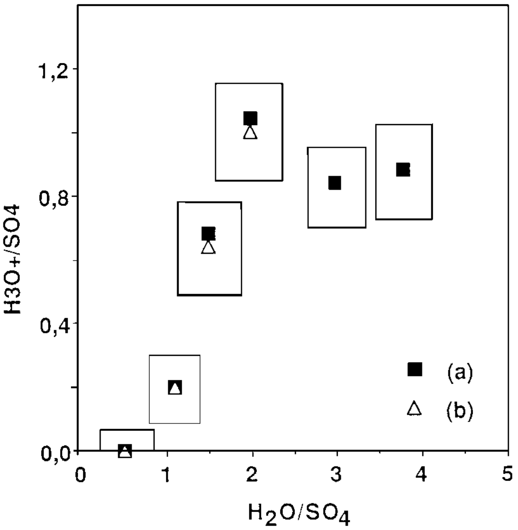

FIG. 5. Plot of H_3O^+/SO_4 versus ads. H_2O/SO_4, (a) using the three-spin isosceles configuration to describe possible interactions between OH groups and water molecules, (b) assuming no first-order magnetic interaction between H atoms of OH groups and of water molecules (see text).

characteristic of water molecules, the other for OH groups (Fig. 2B and Tables 1 and 2). However, such new simulations are valid only if they give the same chemical compositions as those using isosceles three-spin configurations, in agreement with Refs. (41 and 42). Table 1 shows that this is indeed the case for the numbers of OH groups and water molecules per SO_4; in particular, the hydroxonium ion concentration is unchanged (Table 1 and Fig. 5).

When ads. H_2O/SO_4 goes from 1.1 to 2.0, H_3O^+/SO_4 increases from 0.23 ± 0.02 to 1.05 ± 0.10. For higher ads. H_2O/SO_4 the situation is the following (Tables 1 and 2 and Fig. 5): (i) H_3O^+/SO_4 levels off (Fig. 5); (ii) the r' distance parameter for the $H_2O \cdots HO$ species indicates that each acidic OH group which was not transformed into hydroxonium ion is weakly hydrogen-bonded to a water molecule; (iii) some "free" water molecules, not interacting with OH groups, are present (denoted "residual H_2O" in Tables 1 and 2) (Fig. 4); (iv) a few OH groups (about 0.4 per SO_4) remain.

DISCUSSION

As we have already stated, acid strength cannot be determined from the chemical shift of the acidic OH group signal of solids when they are not interacting with a base. For example, the chemical shift of the main signal of pretreated sulfated zirconia at 5.8 ppm is smaller than that of anhydrous Nafion-H (10.6 ppm) (44), which is considered to be strongly acidic, and that of the weakly acidic potassium monohydrogen sulfate (13.5 ppm) (45); however, it is greater than that of bridging acidic OH groups in H-form zeolites (3.8–5.2 ppm) (31–35), solids which are used as strong acid catalysts.

As soon as water is adsorbed on sulfated zirconia pretreated in vacuum, the broad signal of the ^{1}H MAS spectra which replaces the main one in the anhydrous sample (at 5.8 ppm) corresponds, as for zeolites (31, 32, 35), to chemically exchanging H atoms of the oxyprotonated species of Fig. 1 equilibrated at 300 K. It is likely that they are exchanging only between the surface sites where all the sulfated species are assumed to be. The chemical shift δ_E of this signal depends on ads. H_2O/SO_4. It should be remembered that typical ^{1}H chemical shifts are 4.8 ppm for water clusters (35) and 9–13 ppm for hydroxonium ions (44) depending on the hydrogen bonds that they form. The change in chemical shift agrees qualitatively with the broad-line results: (i) δ_E first decreases when water is adsorbed, in agreement with the broad-line results that water does not interact with OH groups (Table 1, ads. $H_2O/SO_4 = 0.50$); (ii) δ_E then increases to a maximum value (7 ppm) for ads. $H_2O/SO_4 = 2$, when the relative concentration of H atoms in hydroxonium ions (50%) is maximum; (iii) δ_E decreases for larger values of ads. H_2O/SO_4 when the residual H_2O/SO_4 concentration increases (Table 1).

The H atoms corresponding to the shoulder at about 9 ppm (Fig. 3C) can probably be attributed to HSO_4^- ions not exchanging with others. Their chemical shift is in acceptable agreement with the 13.5 ppm value found by Mastikhin *et al.* (45) for $KHSO_4$, if we consider that such large chemical shifts are due to hydrogen bond formation between HSO_4^- ions and O atoms; however, the ions cannot be hydrogen-bonded to water O atoms, since the broad-line results indicate that they do not interact. The 9 ppm signal is no longer present in the MAS spectrum for ads. H_2O/SO_4 larger than 2 (Fig. 3D). Let us consider the isosceles three-spin magnetic configuration used to simulate these HSO_4^- ions assumed to be interacting with water; the r' value found was too large for interaction when ads. $H_2O/SO_4 \leq 2$ but, for ads. $H_2O/SO_4 > 2$, it decreased: weak hydrogen bonds could exist between HSO_4^- ions and water; the H atoms of HSO_4^- ions then probably take part in the chemical exchange.

The results of the broad-line experiment show that, when water molecules are adsorbed on pretreated sulfated zirconia, hydroxonium ions can be formed, their maximum concentration, about 1 per SO_4 group, being attained when ads. H_2O/SO_4 is 2 (Fig. 5). Ranking sulfated zirconia on the Brønsted acidity scale proposed for solids (33) gives a mean ionization coefficient, α_a (defined as the hydroxonium ion concentration per Brønsted acid site (denoted bas) when ads. H_2O/bas = 1), equal to 0.5. This value is larger than those obtained to date for zeolites [0.2 for Y zeolites (32) and ZSM-5 (46), 0.33 for mordenites (47)] but smaller than that for Nafion (about 1) (44).

That H_3O^+/SO_4 should be 1 for ads. $H_2O/SO_4 = 2$ recalls immediately the first high pK_a, about −9, of sulfuric acid in aqueous solution. The second pK_a, 2, of sulfuric acid under the same conditions is low, in agreement with our result which shows no interaction between H_2O and the second acidic OH group of the sulfated zirconia (the O–O distance would be about 300 pm if the system were hydrogen-bonded). Therefore, it seems reasonable to consider that there is a distinct α_a value for each of the two OH groups per SO_4 of sulfated zirconia. When ads. H_2O/SO_4 is 2 (one water molecule per OH group) α_a should be 1 and 0 for the first and second OH groups, respectively. However, it must be noted that these values are not in agreement with the α_a definition which assumes that there is one water molecule per OH group to be tested, belonging to characteristic OH group type (33). If we consider the two OH groups of one H_2SO_4 on the zirconia surface as different types, H_3O^+/SO_4 should be 1 for ads. $H_2O/SO_4 = 1$ instead of 2. However, for ads. $H_2O/SO_4 = 1$, the value of H_3O^+/SO_4 value is only 0.27. No hydroxonium ions were found for ads. $H_2O/SO_4 = 0.5$. As for H_2SO_4 itself, the meaning of these results is that the acidities of the two OH groups of a given SO_4 group are not independent.

Our conclusions are consistent with those of Babou *et al.* (48). These authors, working on samples prepared like ours, identified adsorbed H_2SO_4 species and HSO_4^- ions by IR. The sulfated species on the surface of the vacuum pretreated sample seems indeed to be bonded H_2SO_4. The pretreatment conditions do not dehydroxylate this sulfuric acid. The HSO_4^- ions, observed after increasing water adsorption, are formed at the same time as H_3O^+. In agreement with Babou *et al.* (48), our final result is that the acidity of sulfated zirconia corresponds roughly to that of pure H_2SO_4, i.e., the material is not really a superacid, which implies that it is more acidic than H_2SO_4.

CONCLUSION

The interaction of water with a sulfated zirconia, optimized for isomerization of *n*-butane (4), has been studied by two ^{1}H NMR techniques: MAS at 300 K and broad-line at 4 K. The two techniques give results in good agreement. The surfaces of the samples evacuated at 570 K being covered with a monolayer of adsorbed H_2SO_4 species (4), the adsorption of two water molecules per SO_4 group gives one hydroxonium ion per SO_4. The water molecule not involved in hydroxonium ion formation does not hydrogen bond the HSO_4^- group unless the adsorbed water molecule concentration per SO_4 group is >2. For numbers of adsorbed water molecule per SO_4 equal to or larger than 2, the hydroxonium ion concentration is unchanged. Applying the criteria that we proposed to define a scale of Brønsted acidity for solids (33), we obtain a mean ionization coefficient, α_a, of 0.5, larger than for zeolites but smaller than for Nafion.

REFERENCES

1. Olah, G. A., Surya Prakash, G. K., and Sommer, J., "Superacids," p. 54. Wiley, New York, 1985.
2. Tanabe, K., Misono, M., Ono, Y., and Hattori, H., *Stud. Surf. Sci. Catal.* **51**, (1989).
3. Hino, M., and Arata, K., *J. Chem. Soc. Chem. Comm.* 851 (1980).
4. Chen, F. R., Coudurier, G., Joly, J. F., and Védrine, J., *J. Catal.* **143**, 616 (1993).
5. Matsuhashi, H., Motoi, H., and Arata, K., *Catal. Lett.* **26**, 325 (1994).
6. Sohn, J. R., and Jang, H. J., *J. Mol. Catal.* **64**, 349 (1991).
7. Guo, C., Yao, S., Cao, J., and Qian, Z., *Appl. Catal. A,* **107**, 229 (1994).
8. Morterra, C., Cerrato, G., Emanuel, C., and Bolis, V., *J. Catal.* **142**, 349 (1993).
9. Morterra, C., Cerrato, G., Pinna, F., Signoretto, M., and Strukul, G., *J. Catal.* **149**, 181 (1994).
10. Afanasiev, P., Geantet, C., and Breysse, M., *J. Mater. Chem.* **4**, 1653 (1994).
11. Ward, D. A., and Ko, E. I., *J. Catal.* **150**, 18 (1994).
12. Strydom, C. A., and Pretoruius, G., *Thermochim. Acta* **223**, 223 (1993).
13. Chokkaram, S., Srinivasan, R., Milburn, D. R., and Davis, B. H., *J. Colloid Interf. Sci.* **165**, 160 (1994).
14. Riemer, T., Spielbauer, D., Hunger, M., Mekhemer, G. A. H., and Knözinger, H., *J. Chem. Soc.,Chem. Commun.* 1181 (1994).
15. Yamaguchi, T., Jin, T., Ishida, T., and Tanabe, K., *Mater. Chem. Phys.* **17**, 3 (1987).
16. Bensitel, M., Saur, O., Lavalley, J. C., and Morrow, B. A., *Mater. Chem. Phys.* **19**, 147 (1988).
17. Waqif, M., Bachelier, J., Saur, O., and Lavalley, J. C., *J. Mol. Catal.* **72**, 127 (1992).
18. Nascimento, P., Akratopoulou, C., Oszagyan, M., Coudurier, G., Travers, C., Joly, J. F., and Védrine, J., *Stud. Surf. Sci. Catal.* **75**B, 1185 (1993).
19. Morterra, C., Cerrato, G., and Bolis, V., *Catal. Today,* **17**, 505 (1993).
20. Morterra, C., Bolis, V., Cerrato, G., and Magnacca, G., *Surf. Sci.* **307–309**, 1206 (1994).
21. Ebitani, K., Hattori, H., and Tanabe, K., *Langmuir* **6**, 1743 (1990).
22. Kustov, L. M., Kazansky, V. B., Figueras, F., and Tichit, D., *J. Catal.* **150**, 143 (1994).
23. Pinna, F., Signoretto, M., Strukul, G., Cerrato, G., and Morterra, C., *Catal. Lett.* **26**, 339 (1994).
24. Corma, A., Fornés, V., Juan-Rajadell, M. I., and Lopez Nieto, J. M., *Appl. Catal. A* **116**, 151 (1994).
25. Morterra, C., Cerrato, G., Pinna, F., and Signoretto, M., *J. Phys. Chem.* **98**, 12373 (1994).
26. Parera, J. M., *Catal. Today* **15**, 481 (1992). [and references therein]
27. Chen, F. R., Coudurier, G., Joly, J. F., and Védrine, J., "Proceedings New York ACS Meeting, Division of Petroleum Chemistry," Vol. 36. 1993.
28. Mastikhin, V. M., Mudrakovsky, I. L., and Nosov, A. V., *Prog. Nucl. Magn. Res. Spectrosc.* **23**, 259 (1991).
29. Lunsford, J. H., Sang, H., Campbell, S. M., Liang, C. H., and Anthony, R. G., *Catal. Lett.* **27**, 305 (1994).
30. Babou, F., Bigot, B., and Sautet, P., *J. Phys. Chem.* **97**, 11501 (1993).
31. Batamack, P., Dorémieux-Morin, C., Fraissard, J., and Freude, D., *J. Phys. Chem.* **95**, 3790 (1991).
32. Batamack, P., Dorémieux-Morin, C., and Fraissard, J., *J. Chim. Phys.* **89**, 423 (1992).
33. Batamack, P., Dorémieux-Morin, C., Vincent, R., and Fraissard, J., *J. Phys. Chem.* **97**, 9779 (1993).
34. Freude, D., *Stud. Surf. Sci. Catal.* **52**, 169 (1989). [and references therein]
35. Pfeifer, H., and Ernst, H., *Annu. Rep. NMR Spectrosc.* **28**, 91 (1994). [and references therein]
36. Haupt, J., *Phys. Lett.* **38**A, 389 (1972).

37. Pake, G. E., *J. Chem. Phys.* **16**, 327 (1948).
38. Andrew, E. R., and Bersohn, R. J., *J. Chem. Phys.* **18**, 159 (1950).
39. Richards, R. E., and Smith, J. A. S., *Trans. Faraday Soc.* **48**, 675 (1952).
40. Andrew, E. R., and Finch, N. D., *Proc. Phys. Soc.* **70**B, 980 (1957).
41. Dorémieux-Morin, C., *J. Magn. Res.* **21**, 419 (1976).
42. Dorémieux-Morin, C., *J. Magn. Res.* **33**, 505 (1979).
43. Porte, A. L., Gutowsky, H. S., and Boggs, J. E., *J. Chem. Phys.* **36**, 1695 (1962).
44. Batamack, P., and Fraissard, J., *Catal. Lett.* **35**, 135 (1995).
45. Mastikhin, V. M., and Nosov, A. V., personal communication.
46. Heeribout, L., Batamack, P., Dorémieux-Morin, C., Vincent, R., and Fraissard, J., "Colloids and Surfaces A: Physicochemical and Engineering Aspects," Submitted for publication.
47. Heeribout, L., Semmer, V., Batamack, P., Dorémieux-Morin, C., Fraissard, J., and Antos, G., *J. Chem. Soc. Faraday Trans.* **91**, 3933 (1995).
48. Babou, F., Bigot, B., Coudurier, G., Sautet, P., and Védrine, J., *in* "Acid–Base Catalysts II" (H. Hattori, Ed.), p. 519. Kodansha, Tokyo, 1994.